# Endoscopic Endonasal Approach to the Infratemporal Fossa

22

Stefan Lieber and Sébastien Froelich

**Abstract**

The infratemporal and pterygopalatine fossae are anatomically and functionally linked and highly significant for skull base surgery and other specialties including otolaryngology, ophthalmology, maxillofacial surgery, and radiation oncology due to their central location and their extensive connections with neighboring skull base regions. Endoscopic surgery is rendered possible by advanced endoscopic instrumentation, dependable strategies for closure and reconstruction, and an intimate knowledge of the surgical anatomy; this holds particularly true for the complex anatomical contents of the pterygopalatine and infratemporal fossae. Four figures have been included in this chapter with the aim to provide a review of the relevant anatomy, to identify reliable surgical landmarks, and to illustrate the surgical steps of the expanded endoscopic endonasal transpterygoid-transmaxillary approach to the pterygopalatine and infratemporal fossae (Figs. 22.1, 22.2, 22.3, and 22.4).

**Keywords**

Endoscopic endonasal approach · Transpterygoid approach · Transmaxillary approach · Infratemporal fossa · Pterygopalatine fossa · Skull base · Coronal plane · Maxillary artery · Sphenopalatine artery · Medial maxillectomy · Transantral approach · Trigeminal schwannoma · Juvenile angiofibroma · Sinonasal carcinoma

S. Lieber (✉) · S. Froelich
Department of Neurosurgery, Lariboisière Hospital, University of Paris, Paris, France
e-mail: Stefan.Lieber@aphp.fr

## 22.1 Introduction

The infratemporal fossa (ITF) is a deep-seated, retromaxillary space that contains the pterygoid muscles, the maxillary artery with its branches, the mandibular division of the trigeminal nerve with its branches, the otic ganglion, and the pterygoid venous plexus [1–8]. It is bounded by the lateral pterygoid plate medially, the posterolateral surface of the maxillary sinus anteriorly, the infratemporal crest laterally, and the mandibular fossa posterolaterally. The roof of the infratemporal fossa is formed by the greater wing of the sphenoid bone, posteromedially it is separated from the postyloid compartment of the parapharyngeal space by the stylopharyngeal and sphenopharyngeal fasciae; the plane of these fasciae largely corresponds to the petrosphenoidal fissure.

Functionally and anatomically, the infratemporal fossa is closely linked to the pterygopalatine fossa (PPF), a small space in the shape of an inverted quadrangular pyramid, which is located at the angle of the inferior orbital and pterygomaxillary fissures. The pterygopalatine fossa accommodates terminal branches of the maxillary artery, the Vidian nerve, the maxillary division of the trigeminal nerve, and the pterygopalatine ganglion. The pterygopalatine fossa represents a critical crossroad of the skull base as it communicates with the orbit (via the orbital apex and the posteromedial segment of the inferior orbital fissure), the nasal cavity (via the sphenopalatine foramen), the middle cranial fossa (via the foramen rotundum, and the Vidian canal), the nasopharynx (via the palatosphenoidal canal), and the oropharynx (via the greater and lesser pterygopalatine canals). It is in continuum with the infratemporal fossa through the pterygomaxillary fissure which in turn communicates with the orbit (via the anteromedial segment of the inferior orbital fissure), the middle cranial fossa (via the foramen ovale, spinosum, and venosum Vesalii), and the parapharyngeal space [9–17]. Pathological processes and neoplasms can arise primarily or extend into the infratemporal fossa from these adjacent



T. L. POON et al. (eds.), *Orbital Apex and Periorbital Skull Base Diseases*, https://doi.org/10.1007/978-981-99-2989-4_22

regions and include vascular tumors such as juvenile nasopharyngeal angiofibroma and hemangiopericytoma, meningioma with extracranial extension, schwannoma originating primarily from the extracranial portion of the mandibular nerve, lymphoproliferative disorders, and sinonasal carcinoma [18–20].

Numerous surgical corridors to the infratemporal fossa have been described, among them the anterior transmaxillary approach (Le Fort I and II osteotomies with a sublabial or facial incision), the transmandibular approach (requiring a facial degloving), the transcranial extension of the fronto-temporo-orbito-zygomatic approach (through the anterolateral triangle and the middle cranial fossa floor), and the lateral transtemporal approaches (Fisch type A-C) [21–28]. While a comprehensive review of all these approaches is beyond the scope of this chapter, some are discussed elsewhere in this volume (Chap. 22: transcranial approaches, and Chap. 25: endoscopic transorbital approaches).

This chapter addresses the endoscopic endonasal approach to the pterygopalatine and infratemporal fossae. Expanded endoscopic approaches (EEA) have become an important part in the armamentarium of skull base surgeons and can be classified into approach modules in the sagittal plane (craniocaudal) and coronal plane (medio-lateral).

Extended endoscopic approaches to the paramedian skull base, including the transpterygoid-transmaxillary approach to the PPF and ITF, are approaches of minimal access but rarely of minimally invasiveness [6, 19]. However, they avoid the cosmetic and (at least partially) the functional morbidity associated with more traditional open approaches, shorten postoperative recovery time, and thereby accelerate transition to adjuvant radiotherapy. EEAs provide a well-illuminated, magnified, and multiangled view for safe and effective manipulation of tissues in a deep-seated region, and thereby maximize the probability of complete resection.

The expanded transpterygoid-transmaxillary approach entails the following steps:

- Exposure of the maxillary sinus
- Identification of the sphenopalatine artery
- Removal of the posterior wall of the maxillary sinus
- Removal of the perpendicular plate and the pyramidal process of the palatine bone
- Exposure of the periosteum wrapping the content of the pterygopalatine fossa
- Identification of the Vidian and maxillary nerve
- Identification of vascular structures (branches of the maxillary artery)
- Transposition or removal of the contents of the pterygopalatine fossa
- Removal of the pterygoid base with transposition or transection of the Vidian nerve
- Closure and reconstruction

## 22.2 Principles of Approach Selection, Modifications, and Limitations

Although the initial steps are similar, each surgical target requires slight modification to the endoscopic endonasal transpterygoid-transmaxillary approach for access to the PPT and ITF. These modifications largely depend on the topography, morphology, and anticipated pathology of the targeted lesion, the patient's individual anatomy and preexisting loss of function, and the skull base surgeon's preference and experience.

For resection of malignant tumors, adequate surgical exposure should not be compromised by efforts to limit the invasiveness of the approach or by concerns for subsequent loss of sinonasal function since insufficient maneuverability, and loss of visualization and control over tumor margins invariably hampers oncologic integrity of the resection [18–20].

The addition of a posterior septectomy has various advantages: first, it is the prerequisite for a binostril, 2-surgeon, 4-hand technique. Second, it permits the elevation of a nasoseptal flap on the contralateral side for later reconstruction since the vascular pedicle on the ipsilateral side is usually sacrificed during the approach. Third, it greatly improves angulation and therefore lateral reach. Access lateral to the infraorbital nerve is possible with a maxillary antrostomy, modified medial maxillectomy, or total maxillectomy in 63.3% of cases; this is improved to 97.6% when a posterior transseptal approach is used [18].

While the PPF can be reached by limited endoscopic approaches such as the medial transpalatine approach (for the medial aspect of the PPF) or a middle meatal transantral approach (for a more lateral exposure where the infraorbital nerve is the first landmark to be identified), lateral access to the ITF usually requires at least an inferior turbinectomy and a modified medial maxillectomy. The lateral pterygoid plate is considered the lateral boundary accessible via a purely endonasal approach, further lateral and posterior reach is limited by the nasal osseous pyramid and the nasolacrimal canal.

In addition to the use of angled endoscopes and instruments, the exposure of the posterior and posterolateral wall of the maxillary sinus and laterally toward the ITF can be maximized by the following approach modules:

- The addition of a posterior septectomy (as detailed above)
- Using a total rather than a modified medial maxillectomy, where the maxillary sinus is entered anterior to the nasolacrimal duct
- The addition of an endoscopic anterior maxillotomy (Denker's procedure), where the entire medial buttress is removed without the need for a separate sublabial incision

- The addition of a prelacrimal approach, which usually permits to preserve function of the nasolacrimal duct without the need for further reconstruction
- The addition of a Caldwell-Luc approach, an anterior transmaxillary approach through the canine fossa with a sublabial incision (providing direct lateral access and permitting removal of anteriorly based lesions in the maxillary sinus)
- The combination of some of these approach adjuncts, e.g., access via a contralateral transmaxillary corridor

Major challenges of the endoscopic endonasal transpterygoid-transmaxillary approach remain the technical difficulty in controlling hemorrhage from the abundant and highly variable vasculature and the limitation in reaching the lateral aspect of the infratemporal fossa.

## 22.3 Surgical Comorbidity

Nasal crusting, impaired sense of olfaction, empty nose syndrome, and bad smell are well-established sequelae of endoscopic endonasal surgery. The transpterygoid-transmaxillary approach and removal of lesions in the PPF and ITF invariably result in sacrifice of functional tissues, and the following postoperative comorbidities are to be expected for this type of surgery; patients need to be counseled accordingly. Sacrifice of the Vidian nerve results in xerophthalmia, which carries the risk of corneal dysfunction, especially in conjunction with functional loss of the ophthalmic branch of the trigeminal nerve. Transection of the descending palatine nerves results in a variety of sensory dysfunctions of the palate (hypoesthesia, anesthesia, or deafferentation pain). Surgical manipulation within the masticator space with partial resection of the lateral and medial pterygoid muscles leads to immediate postoperative muscle swelling or permanent trismus. Facial numbness, oroantral fistulas, recurrent sinusitis, and devitalized teeth can result from the medial access to the maxillary sinus; dacryocystitis can develop due to the disruption of the nasolacrimal duct. Complications related to the Caldwell-Luc approach and Denker's endoscopic maxillotomy include injury to the anterior superior alveolar nerve, the canine roots, and facial deformity. The latter is due to the loss of lateral support of the alar cartilage to the pyriform aperture when the medial buttress is removed during an endoscopic anterior maxillotomy (Denker's procedure).

## 22.4 Surgical Setup

Following the administration of preoperative antibiotics, and disinfection and decongestion of the nasal cavity, the patient's head is secured in a Mayfield head holder. For EEA, we usually position the patient in a slight reverse Trendelenburg with the head elevated to 15° to decrease central venous pressure and to aid hemostasis. An MRI- and CT-based neuronavigation system is referenced, for lesions originating in the orbit, PPF and ITF fat suppressed T1 post-contrast MRI sequences are useful due to the high content of fat in these regions. Neuromonitoring for the relevant cranial nerves is installed.

If the harvest of autologous tissue for reconstruction or obliteration of a resection cavity is anticipated (e.g., abdominal fat, fascia lata, temporoparietal flap), the respective surgical sites are prepared accordingly. We use angled endoscopes (30° and 45°) for all skull base procedures including the nasal stage because of the dynamic multidirectional visualization and the minimization of interference between instruments and the endoscope.

## 22.5 Nasal Stage, Access to the Maxillary Sinus, Considerations for Reconstruction (Figs. 22.1 and 22.2)

Expansive lesions often invade, distort, or obliterate normal anatomy that usually guides endoscopic surgery. Following stable anatomic landmarks and establishing the boundaries of the lesion are key principles to ensure safe surgery. In the nasal cavity, nasal floor, posterior choana, Eustachian tube orifice, and nasal crest can aid in orientation [29].

The nasal stage of the endoscopic transpterygoid-transmaxillary approach begins with an uncinectomy, a wide maxillary antrostomy and a sphenoethmoidectomy until the medial wall of the maxillary sinus and its transition into the medial orbital wall (lamina papyracea) is reached. A modified medial maxillectomy is performed and the inferior turbinate resected; its mucosa can be used for a free flap reconstruction. Similarly, a flap from the nasal floor can be harvested and reflected medially. A posterior septectomy is added and the ethmoid's perpendicular plate saved for reconstruction. If a nasoseptal flap is to be harvested, this can be done on the contralateral side and the flap stored in the oropharynx [30–32]. The medial maxillary wall is resected posteriorly to the level of the greater palatine canal and anteriorly to the level of the nasolacrimal duct; the maxillectomy should be flush with the nasal floor to ensure free movement of instruments. The mucosa is elevated from the orbital process of the palatine bone to identify the crista ethmoidalis and to expose the sphenopalatine foramen with the posterior septal and posterior lateral nasal arteries emerging from it; these branches of the maxillary artery are usually coagulated for hemostatic control. The sphenopalatine artery provides 90% of the blood supply to the nasal cavity and commonly branches before exiting the sphenopalatine foramen. Its branches can serve as landmarks to identify the sphenopalatine foramen (toward the PPF), as well as the palatosphenoidal and Vidian canals [33–36].

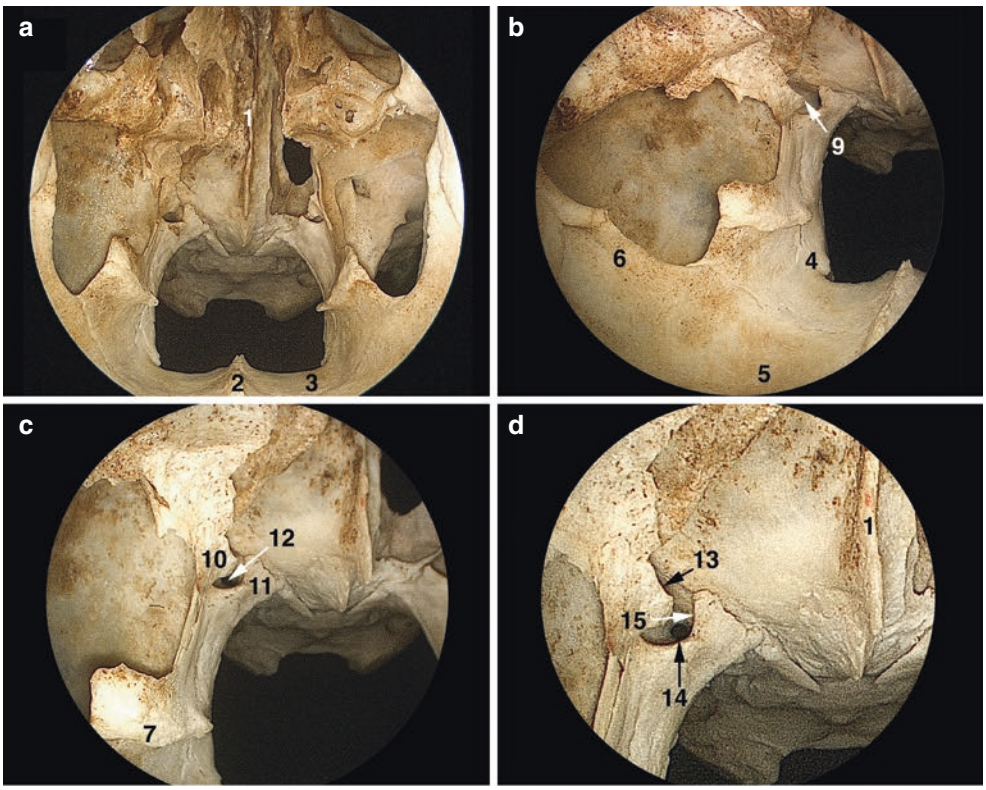


**Fig. 22.1** Osteology, endoscopic endonasal approach to the pterygopalatine and infratemporal fossae. Dry skull specimen. Bilateral maxillary antrostomies and a nasal septectomy have been conducted, on the left side supplemented by a sphenoidotomy and removal of the maxillary sinus' posterior wall. (**a**) The osseous nasal septum consists of the perpendicular plate of the ethmoid bone and the vomer, it inserts at the sphenoidal rostrum (1) and the nasal crest (2). The horizontal plates of each palatine bone (3) merge in the midline to form the posterior part of the hard palate and the nasal crest. (**b**) (view toward the right) The pyramidal process of the palatine bone (4) accommodates the pterygopalatine canal and the greater palatine foramen. The palatine processes of the maxillary bone (5) represent the anterior part of the hard palate. The perpendicular plate of the palatine bone connects anteriorly with the rough surface of the maxillary bone to form the maxillary sinus' medial wall (6); its conchal crest (7) serves as the attachment for the inferior turbinate. (**c**) (zoomed detail of **b**) The middle turbinate belongs to the ethmoid bone, yet the most posterior aspect of its basal lamella blends into the ethmoidal crest of the palatine bone (8) which terminates just anteroinferior to the sphenopalatine foramen (9). (**d**) (zoomed detail of **c**) The anatomy of the palatine bone is central to the understanding of endoscopic endonasal approaches in the coronal plane. Superolaterally, the orbital process (10) attaches to the orbital surface of the maxillary bone, superomedially, the sphenoidal process (11) attaches to the base of the medial pterygoid plate. The orbital and sphenoidal processes are separated by the sphenopalatine notch, which becomes the sphenopalatine foramen when covered by the sphenoid bone superiorly. A shallow recess in the anterior surface of the base of the pterygoid process represents the posterior wall of the pterygopalatine fossa (12) and contains the orifices of the foramen rotundum (13, view obstructed by the orbital process) superolaterally, the Vidian/pterygoid canal (14) posteriorly, and the palatosphenoidal canal (15, view obstructed by the sphenoidal process) medially. The anterior wall of the pterygopalatine fossa is formed by the maxillary bone. (**e**) (view toward the left) The maxillary sinus' posterior wall (16) has been removed to expose the pterygopalatine fossa medially and the infratemporal fossa (17) laterally. (**f**) (more medial view when compared with **e**) The foramen rotundum (13) connects the middle cranial fossa with the pterygopalatine fossa; it opens into its superolateral aspect. The infraorbital canal in the roof of the maxillary sinus is often dehiscent and joins the posteromedial aspect of the inferior orbital fissure. It accommodates the infraorbital nerve (orbitomaxillary segment of the maxillary nerve), which courses posteromedially to enter the pterygopalatine fossa (see also Figs. 22.3 and 22.4. (**g**) (lateral extracranial view onto the left side, posterior wall of the maxillary sinus removed) at the junction of the perpendicular and horizontal plates, the pyramidal process of the palatine bone attaches to the maxillary bone (19) anteriorly and to the oblique inferior margins of the lateral pterygoid plate (20) posterolaterally; the pterygomaxillary fissure (18) lies superior. The pterygoid process of the sphenoid bone connects superiorly to the body and greater wing; it consists of the base and the medial and lateral pterygoid plates. The infratemporal fossa is bounded by the lateral pterygoid plate medially, the posterolateral surface of the maxillary sinus anteromedially, the infratemporal crest (21) laterally, and the mandibular fossa (22) posterolaterally. (**h**) (extracranial view from below, left side) The greater wing of the sphenoid bone (23) forms the roof of the infratemporal fossa, whereas the squamous part of the temporal bone (24) overlies the poststyloid compartment of the parapharyngeal space. In the pterygoid fossa, the depression between the medial and lateral (20) pterygoid plates, an inconstant foramen venosum Vesalii (25) can be found, more posterolaterally and anterior to the petrosphenoidal fissure (26), foramen ovale (27) and foramen spinosum (28) are located

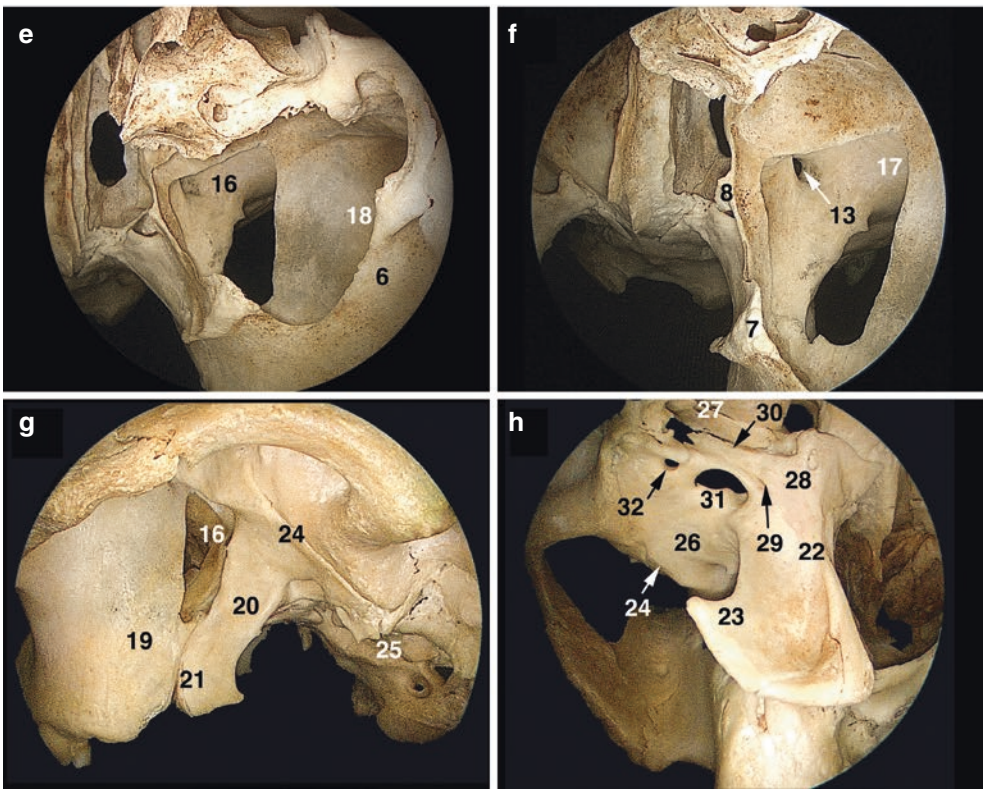


**Fig. 22.1** (continued)

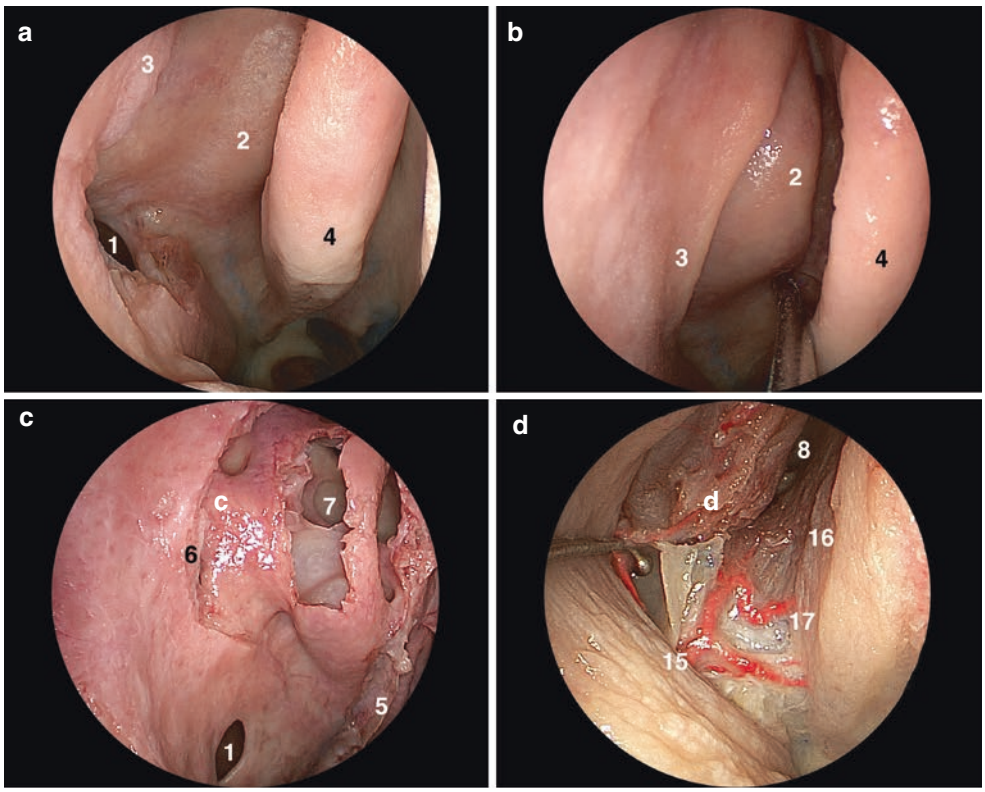


**Fig. 22.2** Nasal stage, terminal branches of the maxillary and sphenopalatine arteries. Color-injected, fixed specimen. (**a**–**f**) right side, (**g**, **h**) left side. (**a**) The maxillary ostium (1) is located inferior to the bulla ethmoidalis (2) and is partially covered by the inferior aspect of the uncinate process (3). (**b**) The middle turbinate (4) is medialized to expose the medial wall of the maxillary sinus and the afore mentioned structures. (**c**) View after middle turbinectomy (5 showing the residual of its basal lamella), uncinectomy (6), and partial ethmoidectomy (7). (**d**) The sphenoidal ostium (8) opens into the sphenoethmoidal recess (9). The sphenopalatine artery represents a terminal branch of the pterygopalatine segment of maxillary artery, it divides into the posterior lateral nasal artery and the posterior septal artery within the pterygopalatine fossa, both branches exit into the nasal cavity via the sphenopalatine foramen. The posterior septal artery (10) courses on the anterior wall of the sphenoid sinus (11) between the sphenoidal ostium and the choana to reach the posterior aspect of the nasal septum; it usually divides into a superior and inferior branch. The inferior turbinate is supplied by a branch of the posterior lateral nasal artery (12). (**e**) The mucosa overlying the ethmoidal crest (13) has been elevated to expose the sphenopalatine foramen and the posterior lateral nasal and the posterior septal arteries emerging from the pterygopalatine fossa (14). (**f**) The terminal segment of the pterygopalatine segment of maxillary artery (16) bifurcates into the sphenopalatine artery (17) and the descending palatine arteries (18). The sphenopalatine artery then branches into the posterior lateral nasal artery (12) and the posterior septal artery (10). Direct branches can often be identified such as the artery of the foramen rotundum (19), the Vidian artery, or the palatosphenoidal arteries; they emerge variably from the pterygopalatine segment of maxillary artery. (**g**, **h**) If a nasoseptal flap (20) is to be harvested, this is usually done on the contralateral side since its vascular pedicle consisting of the inferior and superior posterior septal arteries (10), would be sacrificed during the surgical approach to the pterygopalatine fossa. The harvested flap can be stored in the nasopharynx (21) or the contralateral maxillary antrum

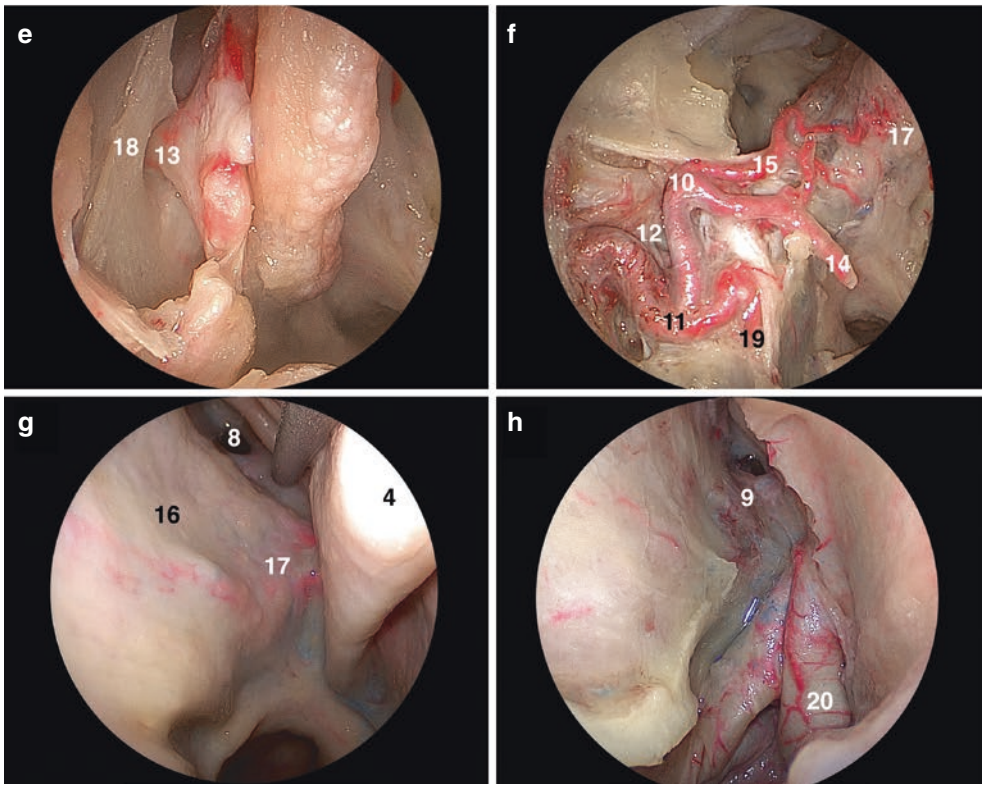


**Fig. 22.2** (continued)

## 22.6 Pterygopalatine Fossa (Figs. 22.1, 22.2, and 22.3)

Drilling continues through the perpendicular plate of the palatine bone, the descending greater and lesser palatine nerves and their artery usually need to be transected for transposition of the PPF contents. The medial pterygoid plate and muscle lie just posterior. The sphenopalatine foramen is largely formed by the orbital and sphenoidal processes of the palatine bone, these can be reduced to expose the pterygopalatine fossa in a medial to lateral direction. The fibrous tissues encountered superolaterally correspond to the Mueller muscle, which is a vestigial muscle surrounded by a thin periosteal sheath that covers the posteromedial segment of the inferior orbital fissure and separates the pterygopalatine fossa from the orbit; manipulation should be minimized to not disrupt postganglionic fibers coursing into the orbit [37, 38]. Once the mucosa is elevated off the maxillary sinus, the infraorbital artery and nerve are readily visualized coursing anterosuperior toward the floor of the orbit. Further resection of the posterior wall of the maxilla exposes the periosteum of the pterygopalatine and infratemporal fossae [39].

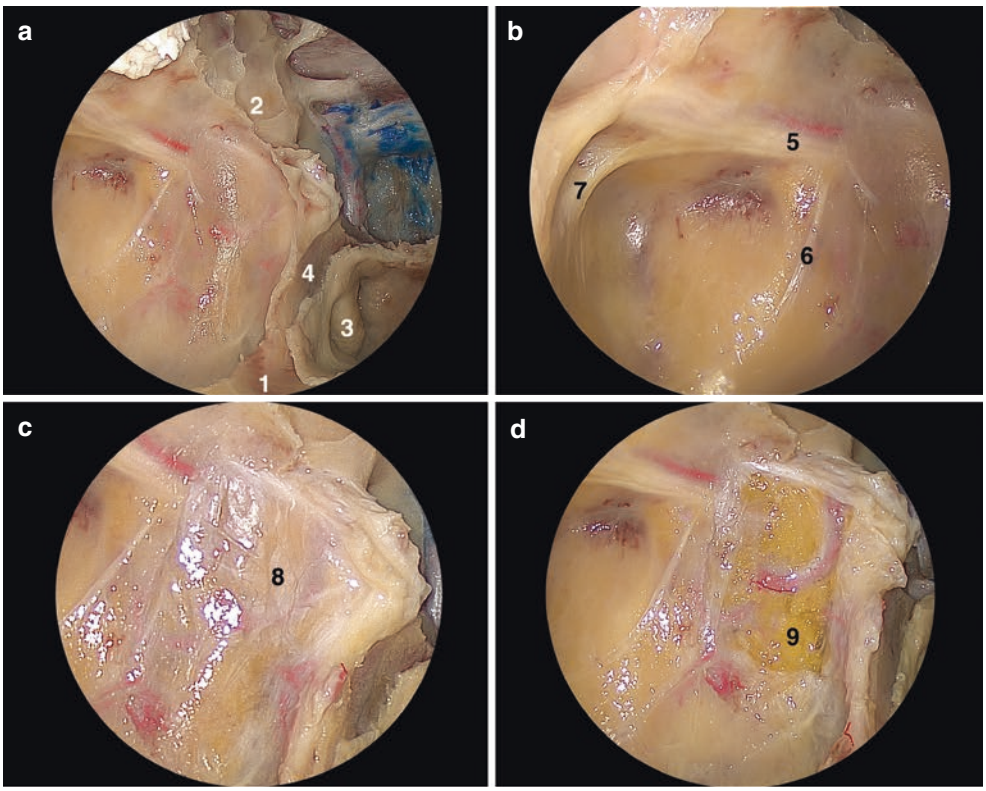


**Fig. 22.3** Pterygopalatine and infratemporal fossae I. Color-injected, fixed specimen. Stepwise exposure, right side. (**a**) View following removal of the maxillary sinus' medial wall (medial maxillectomy), from the level of the hard palate (1) inferiorly to the lamina papyracea (2) superiorly. The torus tubarius (3), the nasopharyngeal ostium of the Eustachian tube, is located posterior to the perpendicular plate of the palatine bone (4). (**b**) Removal of the mucosa reveals the infraorbital nerve and artery (5). The orbitomaxillary segment of the infraorbital nerve gives off the middle superior (6) and the anterior superior alveolar nerves (7) which descend on the maxillary tuberosity. (**c**) Removal of the thin maxillary sinus' posterior wall exposes the subjacent periosteum (8). (**d**) Incision of the periosteum reveals a fat pad (9) that overlies the pterygopalatine and infratemporal fossae. Within this fat pad, the pterygopalatine fossa is organized in two distinct compartments: a superficial vascular compartment and a deep neural compartment. (**e**, **f**) Lateral dissection exposes contents of the pterygopalatine and infratemporal fossae. The junction of the infraorbital canal (10) and the maxillary sinus' posterior wall is just medial to the vertical fibers of the temporalis muscle (11); this point can be used as a landmark to divide the infratemporal fossa and the pterygopalatine fossa from the endoscopic perspective. The pterygopalatine ganglion consists of an assortment of parasympathetic, sympathetic, and somatosensory nerve fibers that regulate secretomotor functions to and provide sensation from various structures including lacrimal glands, and mucous membranes of the oropharynx, nasopharynx, nasal cavity, and the oral cavity. Pterygopalatine segment of the maxillary nerve (12), infraorbital nerve and artery (5), greater and lesser palatine nerves and artery (13), and middle superior alveolar nerve (6). (**g**) Detail of the posterior aspect of the pterygopalatine fossa. The maxillary nerve enters superolaterally via the foramen rotundum (14), while the Vidian nerve enters posteriorly via the Vidian/pterygoid canal (15). The pneumatized lateral recess of the sphenoid sinus (16) belongs to the pterygoid bone. Mueller's muscle (17) covers the inferior orbital fissure and serves as a landmark between orbit and pterygopalatine fossa. The zygomatic nerve (18) courses into Muller's muscle, essentially dividing it into a superior and an inferior part. (**h**) Detail of the perpendicular plate (4) and the descending greater and lesser palatine nerves (13). For details on the pterygopalatine segment of the maxillary artery see Fig. 22.2

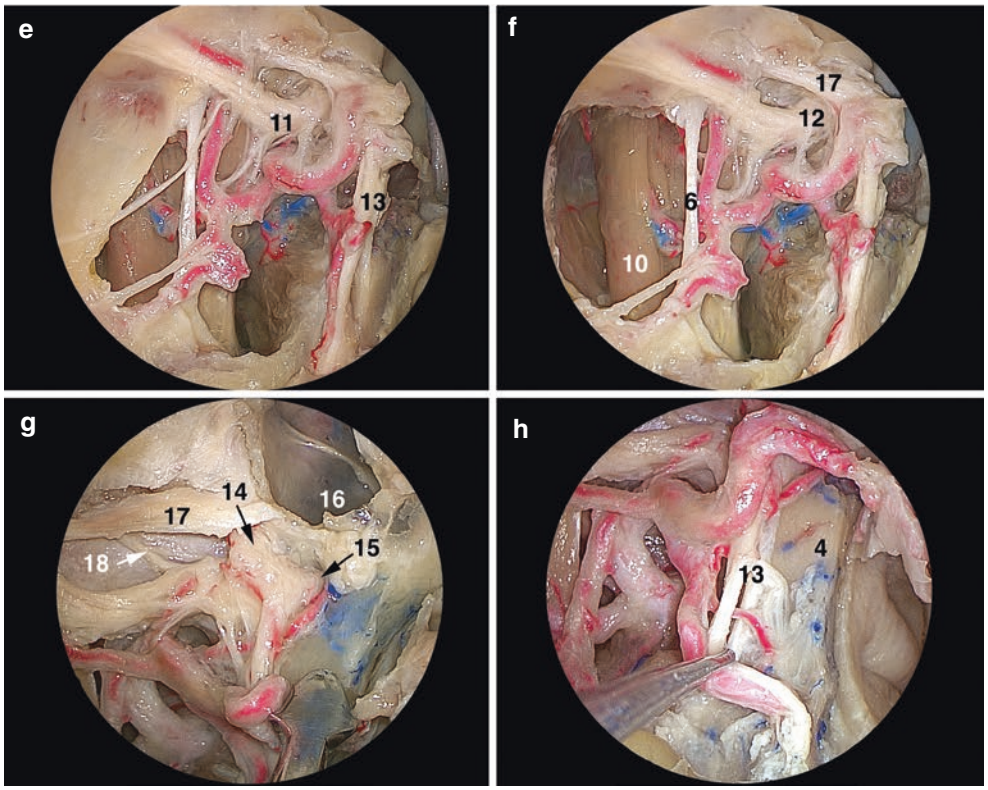


**Fig. 22.3** (continued)

The contents of the pterygopalatine fossa are organized in two distinct compartments: gentle dissection of the fat at first exposes the superficial vascular compartment. The vascular compartment contains the pterygopalatine segment of the maxillary artery which traverses the PPF in a characteristic corkscrew loop (coursing anteriorly, medially, then superiorly); its branches are usually encountered prior to the main artery [40]. The neural compartment lies deeper, its most important structures are the pterygopalatine ganglion, the maxillary and infraorbital branches of the trigeminal nerve, the Vidian nerve, and the greater and lesser descending palatine nerves. Three obliquely oriented foramina are consistently found on the posterior aspect of the pterygopalatine fossa: superolaterally the foramen rotundum, medially the Vidian canal, and inferomedially the palatosphenoidal canal [41]. The Vidian nerve is formed by the union of the greater superficial petrosal and the deep petrosal nerves. It is readily identified at the inferolateral aspect of the sphenoid sinus floor at the junction of the sphenoid body and the pterygoid process. The Vidian canal and the fibrous tissues of the pterygosphenoidal fissure serve as excellent surgical guides to identify the lacerum segment of the internal carotid artery if the approach is taken more posteriorly [42, 43]. The transposition of the pterygopalatine fossa contents with preservation of a mobilized Vidian nerve is generally feasible after transection of the greater and lesser descending palatine nerves, in malignant tumors or for extended exposure its sacrifice is necessary.

## 22.7 Infratemporal Fossa (Figs. 22.1, 22.3, and 22.4)

The pterygoid plates can be followed to their base and attachment to the middle cranial fossa. During the endonasal endoscopic transpterygoid-transmaxillary approach, the medial pterygoid muscle can be recognized by fibers coursing in the vertical plane, complete drilling of the perpendicular plate of the palatine bone and the lateral pterygoid plate is required for its exposure. Its two heads descend in a posterior and lateral direction to insert at the medial surface of the ramus and angle of the mandible. The lateral pterygoid muscle, which occupies most of the superior aspect of the ITF, equally consists of two heads: the superior head originates on the infratemporal surface and crest of the greater wing of the sphenoid bone, just posterolaterally of the inferior orbital fissure, its lower head originates from the lateral surface of the lateral pterygoid plate [44]. Both course posterolaterally, their fibers directed in the horizontal plane. The lateral pterygoid plate is the most useful landmark for the location of the

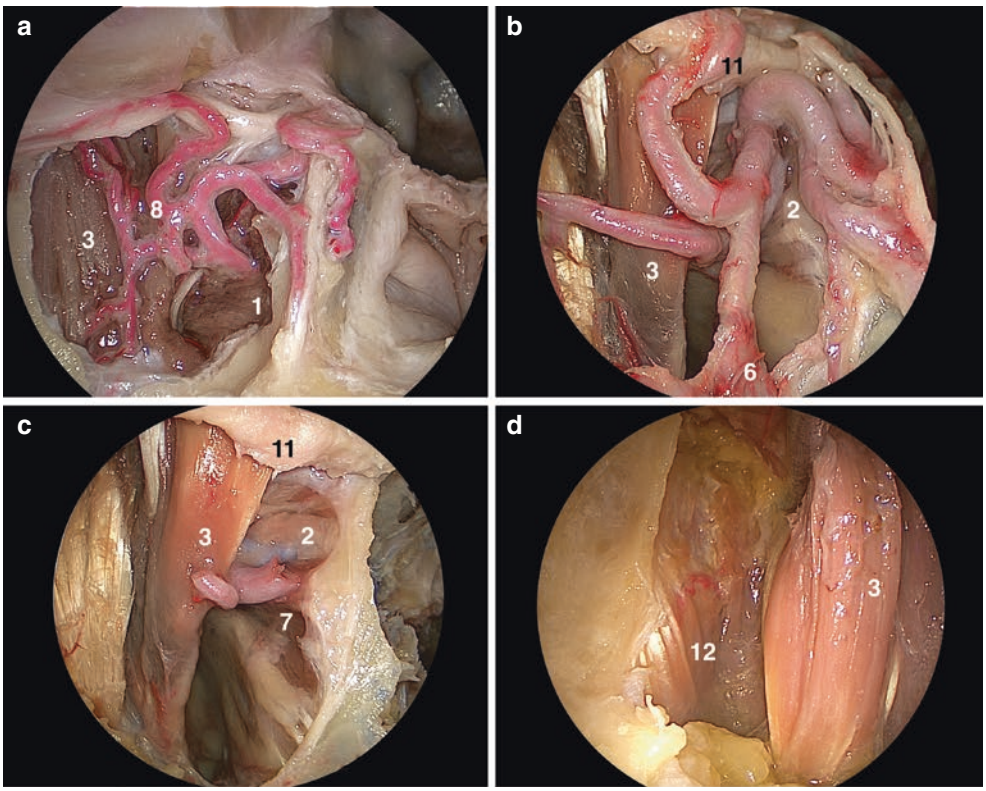


**Fig. 22.4** Pterygopalatine and infratemporal fossae II. Color-injected, fixed specimen. Stepwise exposure, right side. (**a**) The infratemporal fossa is largely occupied by the medial and lateral (1) pterygoid muscles; its lateral boundary is formed by the inner fascia of the temporal muscle (2) which inserts at the infratemporal crest. (**b**) The maxillary artery (3) arises from the external carotid artery and courses anteromedially to enter the infratemporal fossa via an orifice formed by the condylar process of the mandible (4) and the sphenomandibular ligament. There are three named segments to the maxillary artery: mandibular, pterygoid, and pterygopalatine. The mandibular segment spans from the external carotid artery to the lateral aspect of the lateral pterygoid muscle; five branches originate: the deep auricular, anterior tympanic, middle (5) and accessory meningeal, and inferior alveolar arteries. The pterygoid segment continues to the pterygomaxillary fissure; it gives rise to a variable number of muscular branches: the anterior and posterior deep temporal, masseteric, buccal, and pterygoid arteries (see Figs. 22.2 and 22.3 for a description of the pterygopalatine segment). (**c**) The lateral pterygoid muscle consists of two heads: the superior head (1 sup) originates on the infratemporal surface and crest of the greater wing of the sphenoid bone, just posterolateral of the inferior orbital fissure, whereas the lower head (1 inf) originates from the lateral surface of the lateral pterygoid plate. Both course in a posterolateral direction, their fibers directed in the horizontal plane, to inserts at the temporomandibular joint (superior head) and at the condylar process (inferior head). The medial pterygoid muscle passes inferior to the lateral pterygoid muscle on is posterolateral course toward the mandible. Depending on the course of the maxillary artery in relation to the inferior head of the lateral pterygoid muscle, there is a lateral/superficial variant and a medial/deep variant; the latter being less common. (6) perpendicular plate of the palatine bone. (**d**) (extreme lateral view) The masseter muscle (7) is located lateral to the temporalis muscle (2); its fibers oriented in a more oblique direction. (**e**, **f**) The medial pterygoid muscle (not shown) is recognized by fibers coursing in the vertical plane, complete drilling of the perpendicular plate of the palatine bone and the lateral pterygoid plate is required for its exposure from the endonasal perspective. Its smaller superficial head originates from the lateral aspect of the palatine pyramidal process and the maxillary tuberosity, whereas its bigger deep head originates from the medial surface of the lateral pterygoid plate and the pterygoid fossa. The medial pterygoid muscle (8) inserts at the medial surface of the ramus and angle of the mandible (9). The mandibular nerve (10) represents the largest of the three trigeminal divisions; it consists of a sensory root and a smaller motor root. Inferior to the foramen ovale (11), the mandibular nerve courses between the tensor veli palatini muscle and the Eustachian tube (12) posteromedially and the lateral pterygoid muscle anterolaterally; it provides meningeal and muscular branches and then divides into a smaller anterior trunk (13) and a larger posterior trunk (14). The anterior trunk courses laterally just below the roof of the infratemporal fossa; its provides various motor branches (deep temporal, masseteric, pterygoid) and the sensory buccal nerve. The otic ganglion is a peripheral ganglion formed by preganglionic parasympathetic fibers of the lesser petrosal nerve and sympathetic fibers from the plexus on the middle meningeal artery (5); the ganglion is located extracranially just inferior to the foramen ovale (11). The stylopharyngeal fascia originates on the styloid process and the base of the spina sphenoidalis, anterolateral to the external opening of the carotid canal. It blends into the sphenopharyngeal fascia (15) anteromedially to insert at the lateral pterygoid plate. It extends along the anterior aspect of the Eustachian tube and the tensor veli palatini muscle to separate the infratemporal fossa anteriorly from the poststyloid compartment of the parapharyngeal space posteriorly. From the endonasal endoscopic perspective, the Eustachian tube traverses the parapharyngeal space always anterior to the petrous segment of the internal carotid artery. (**g**, **h**) Detail of the region around the foramen ovale. The posterior trunk (14) provides the auriculotemporal nerve (16), as well as the lingual, mylohyoid, and inferior alveolar nerves (not identified in ambiguity). The middle meningeal artery (5) ascends medial to the lateral pterygoid muscle to enter the middle cranial fossa via the foramen spinosum (17). Due to the anteromedial to posterolateral line of sight of the endoscopic approach, the middle meningeal artery is usually found posterior to the mandibular nerve and the foramen ovale. The accessory meningeal artery reaches the middle cranial fossa either via the foramen ovale or the foramen venosum Vesalii

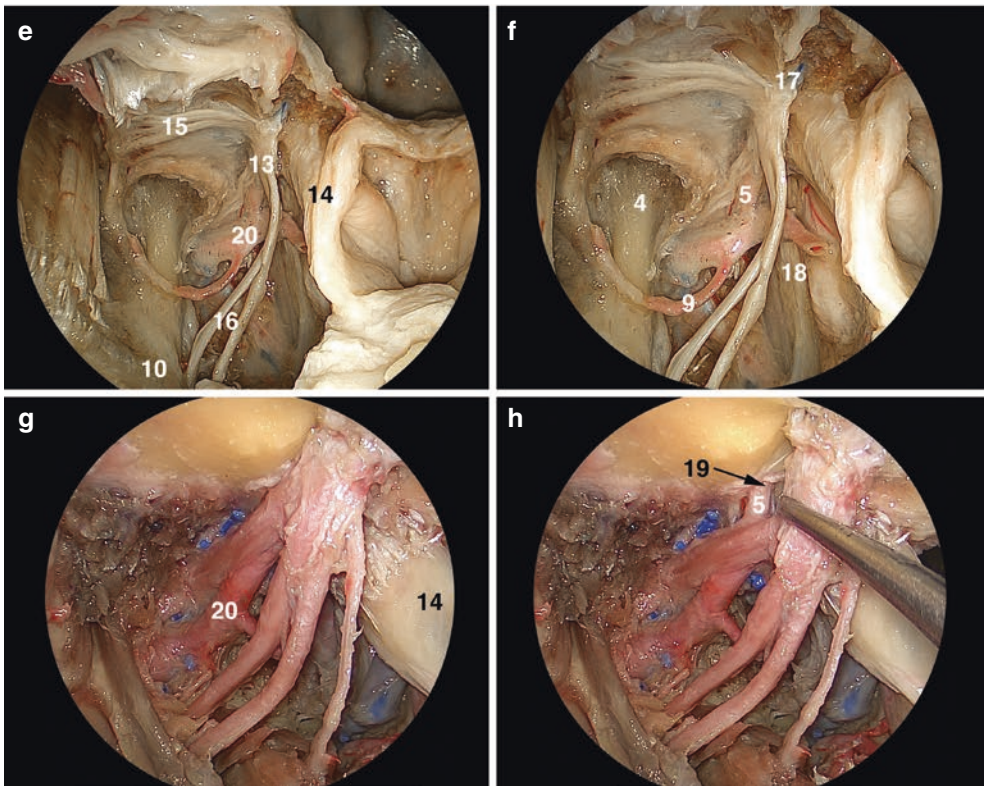


**Fig. 22.4** (continued)

foramen ovale and the mandibular branch of the trigeminal nerve, when drilled flush to the cranial base the foramen ovale is found just posterolateral to it. The foramen spinosum is situated immediately posterolaterally to the foramen ovale, however, due to the anteromedial to posterolateral line of sight of the endoscopic approach, the foramen spinosum is encountered just behind the mandibular nerve as the middle meningeal artery traversing it enters the middle cranial fossa. Alternatively the inferior alveolar nerve can be followed as its courses under the lateral pterygoid muscle toward the foramen ovale [45]. The medial pterygoid plate also serves as the attachment of the superior constrictor muscle of the pharynx and the fibrous raphe to form the lateral layers of the wall of the nasopharynx; its medial plate therefore represents the lateral wall of the nasopharynx [46].

## References

1. Hosseini SMS, Razfar A, Carrau RL, Prevedello DM, Fernandez-Miranda J, Zanation A, Kassam AB. Endonasal transpterygoid approach to the infratemporal fossa: correlation of endoscopic and multiplanar CT anatomy. Head Neck. 2012;34:313–20.
2. Fortes FSG, Sennes LU, Carrau RL, Brito R, Ribas GC, Yasuda A, Rodrigues AJ, Snyderman CH, Kassam AB. Endoscopic anatomy of the pterygopalatine fossa and the transpterygoid approach: development of a surgical instruction model. Laryngoscope. 2008;118:44–9.
3. Theodosopoulos PV, Guthikonda B, Brescia A, Keller JT, Zimmer LA. Endoscopic approach to the infratemporal fossa: anatomic study. Neurosurgery. 2010;66:196–203.
4. Alfieri A, Jho H-D, Schettino R, Tschabitscher M. Endoscopic endonasal approach to the pterygopalatine fossa: anatomic study. Neurosurgery. 2003;52:374–80.
5. Falcon RT, Rivera-Serrano CM, Miranda JF, Prevedello DM, Snyderman CH, Kassam AB, Carrau RL. Endoscopic endonasal dissection of the infratemporal fossa: anatomic relationships and importance of eustachian tube in the endoscopic skull base surgery. Laryngoscope. 2011;121:31–41.
6. Cavallo LM, Messina A, Gardner P, Esposito F, Kassam AB, Cappabianca P, de Divitiis E, Tschabitscher M. Extended endoscopic endonasal approach to the pterygopalatine fossa: anatomical study and clinical considerations. Neurosurg Focus. 2005;19:1–7.
7. Joo W, Funaki T, Yoshioka F, Rhoton AL. Microsurgical anatomy of the infratemporal fossa. Clin Anat. 2013;26:455–69.
8. Daniels DL, Mark LP, Ulmer JL, Mafee MF, McDaniel J, Shah NC, Erickson S, Sether LA, Jaradeh SS. Osseous anatomy of the pterygopalatine fossa. AJNR Am J Neuroradiol. 1998;19:1423–32.
9. Li L, London NR, Prevedello DM, Carrau RL. Anatomy based corridors to the infratemporal fossa: implications for endoscopic approaches. Head Neck. 2020;42:846–53.
10. Elhadi A, Almefty K, Mendes G, Kalani M, Nakaji P, Dru A, Preul M, Little A. Comparison of surgical freedom and area of exposure in three endoscopic transmaxillary approaches to the anterolateral cranial base. J Neurol Surg B Skull Base. 2014;75:346–53.
11. de Lara D, Filho LFSD, Prevedello DM, Carrau RL, Kasemsiri P, Otto BA, Kassam AB. Endonasal endoscopic approaches to the paramedian skull base. World Neurosurg. 2014;82:S121–9.

12. Li L, London NR, Prevedello DM, Carrau RL. Endonasal endoscopic transpterygoid approach to the upper parapharyngeal space. Head Neck. 2020;42:2734–40.
13. DelGaudio JM. Endoscopic transnasal approach to the pterygopalatine fossa. Arch Otolaryngol Head Neck Surg. 2003;129:441–6.
14. Al-Nashar IS, Carrau RL, Herrera A, Snyderman CH. Endoscopic transnasal transpterygopalatine fossa approach to the lateral recess of the sphenoid sinus. Laryngoscope. 2004;114:528–32.
15. Elhadi AM, Zaidi HA, Yagmurlu K, Ahmed S, Rhoton AL, Nakaji P, Preul MC, Little AS. Infraorbital nerve: a surgically relevant landmark for the pterygopalatine fossa, cavernous sinus, and anterolateral skull base in endoscopic transmaxillary approaches. J Neurosurg. 2016;125:1460–8.
16. Labib MA, Belykh E, Cavallo C, et al. The endoscopic endonasal eustachian tube anterolateral mobilization strategy: minimizing the cost of the extreme-medial approach. J Neurosurg. 2021;134:831–42.
17. Hofstetter CP, Singh A, Anand VK, Kacker A, Schwartz TH. The endoscopic, endonasal, transmaxillary transpterygoid approach to the pterygopalatine fossa, infratemporal fossa, petrous apex, and the Meckel cave: clinical article. J Neurosurg. 2010;113:967–74.
18. Oakley GM, Harvey RJ. Endoscopic resection of pterygopalatine fossa and infratemporal fossa malignancies. Otolaryngol Clin North Am. 2017;50:301–13.
19. Snyderman CH, Carrau RL, Kassam AB, Zanation A, Prevedello D, Gardner P, Mintz A. Endoscopic skull base surgery: principles of endonasal oncological surgery. J Surg Oncol. 2008;97:658–64.
20. Tiwari R, Quak J, Egeler S, Smeele L, Waal IV, Valk PV, Leemans R. Tumors of the infratemporal fossa. Skull Base Surg. 2000;10:1–9.
21. Hanakita S, Chang W-C, Watanabe K, Ronconi D, Labidi M, Park H-H, Oyama K, Bernat A-L, Froelich S. Endoscopic endonasal approach to the anteromedial temporal fossa and mobilization of the lateral wall of the cavernous sinus through the inferior orbital fissure and V1-V2 corridor: an anatomic study and clinical considerations. World Neurosurg. 2018;116:e169–78.
22. Shin M, Shojima M, Kondo K, Hasegawa H, Hanakita S, Ito A, Kin T, Saito N. Endoscopic endonasal craniofacial surgery for recurrent skull base meningiomas involving the pterygopalatine fossa, the infratemporal fossa, the orbit, and the paranasal sinus. World Neurosurg. 2018;112:e302–12.
23. Gerges MM, Godil SS, Younus I, Rezk M, Schwartz TH. Endoscopic transorbital approach to the infratemporal fossa and parapharyngeal space: a cadaveric study. J Neurosurg. 2020;133:1948–59.
24. Youssef A, Carrau R, Tantawy A, Ibraheim A, Solares A, Otto B, Prevedello D, Filho L. Endoscopic versus open approach to the infratemporal fossa: a cadaver study. J Neurol Surg B Skull Base. 2015;76:358–64.
25. Alves-Belo JT, Mangussi-Gomes J, Truong HQ, Cohen S, Gardner PA, Snyderman CH, Stefko ST, Wang EW, Fernandez-Miranda JC. Lateral transorbital versus endonasal transpterygoid approach to the lateral recess of the sphenoid sinus—a comparative anatomic study. Oper Neurosurg. 2018;16:600–6.
26. Yan R, Fang X. The endoscopic prelacrimal recess approach to the paramedian middle cranial base: an anatomical study. J Clin Neurosci. 2021;88:251–8.
27. Oyama K, Watanabe K, Hanakita S, Champagne P-O, Passeri T, Voormolen EH, Bernat AL, Penet N, Fukushima T, Froelich S. The orbitopterygoid corridor as a deep keyhole for endoscopic access to the paranasal sinuses and clivus. J Neurosurg. 2020;134(5):1480–9.
28. Watanabe K, Zomorodi AR, Labidi M, Satoh S, Froelich S, Fukushima T. Visualization of dark side of skull base with surgical navigation and endoscopic assistance: extended petrous rhomboid and rhomboid with maxillary nerve–mandibular nerve Vidian corridor. World Neurosurg. 2019;129:e134–45.
29. Rhoton A. Cranial anatomy and surgical approaches. Philadelphia: Lippincott Williams & Wilkins; 2003.
30. Hadad G, Bassagasteguy L, Carrau RL, Mataza JC, Kassam A, Snyderman CH, Mintz A. A novel reconstructive technique after endoscopic expanded endonasal approaches: vascular pedicle nasoseptal flap. Laryngoscope. 2006;116:1882–6.
31. Pinheiro-Neto CD, Paluzzi A, Fernandez-Miranda JC, Scopel TF, Wang EW, Gardner PA, Snyderman CH. Extended dissection of the septal flap pedicle for ipsilateral endoscopic transpterygoid approaches. Laryngoscope. 2014;124:391–6.
32. Fortes FSG, Carrau RL, Snyderman CH, Kassam A, Prevedello D, Vescan A, Mintz A, Gardner P. Transpterygoid transposition of a temporoparietal fascia flap: a new method for skull base reconstruction after endoscopic expanded endonasal approaches. Laryngoscope. 2007;117:970–6.
33. Kim JK, Cho JH, Lee Y-J, Kim C-H, Bae JH, Lee J-G, Yoon J-H. Anatomical variability of the maxillary artery: findings from 100 Asian cadaveric dissections. Arch Otolaryngol Head Neck Surg. 2010;136:813–8.
34. Zhang X, Wang EW, Wei H, Shi J, Snyderman CH, Gardner PA, Fernandez-Miranda JC. Anatomy of the posterior septal artery with surgical implications on the vascularized pedicled nasoseptal flap. Head Neck. 2015;37:1470–6.
35. Tanoue S, Kiyosue H, Mori H, Hori Y, Okahara M, Sagara Y. Maxillary artery: functional and imaging anatomy for safe and effective transcatheter treatment. Radiographics. 2013;33:e209–24.
36. Alvernia JE, Hidalgo J, Sindou MP, Washington C, Luzardo G, Perkins E, Nader R, Mertens P. The maxillary artery and its variants: an anatomical study with neurosurgical applications. Acta Neurochir. 2017;159:655–64.
37. Lieber S, Fernandez-Miranda J. Anatomy of the orbit. J Neurol Surg B Skull Base. 2020;81:319–32.
38. Battista JCD, Zimmer LA, Rodríguez-Vázquez JF, Froelich SC, Theodosopoulos PV, DePowell JJ, Keller JT. Muller's muscle, no longer vestigial in endoscopic surgery. World Neurosurg. 2011;76:342–6.
39. Battista JD, Zimmer L, Theodosopoulos P, Froelich S, Keller J. Anatomy of the inferior orbital fissure: implications for endoscopic cranial base surgery. J Neurol Surg B Skull Base. 2012;73:132–8.
40. Lasjaunias P, ter Brugge KT, Berenstein A. Surgical neuroangiography. 2nd ed. New York: Springer; 2001.
41. Pinheiro-Neto CD, Fernandez-Miranda JC, Rivera-Serrano CM, Paluzzi A, Snyderman CH, Gardner PA, Sennes LU. Endoscopic anatomy of the palatovaginal canal (palatosphenoidal canal). Laryngoscope. 2012;122:6–12.
42. Kassam AB, Vescan AD, Carrau RL, Prevedello DM, Gardner P, Mintz AH, Snyderman CH, Rhoton AL. Expanded endonasal approach: vidian canal as a landmark to the petrous internal carotid artery: technical note. J Neurosurg. 2008;108:177–83.
43. Wang W-H, Lieber S, Mathias RN, Sun X, Gardner PA, Snyderman CH, Wang EW, Fernandez-Miranda JC. The foramen lacerum: surgical anatomy and relevance for endoscopic endonasal approaches. J Neurosurg. 2019;131:1571–82.
44. Lang J. Skull base and related structures. 2nd ed. New York: Schattauer; 2001.
45. Leblanc A. The cranial nerves. 2nd ed. Berlin: Springer.
46. Pinheiro-Neto CD, Fernandez-Miranda JC, Wang EW, Gardner PA, Snyderman CH. Anatomical correlates of endonasal surgery for sinonasal malignancies. Clin Anat. 2012;25:129–34.